ELSEVIER

Surface Science 488 (2001) 239–248

SURFACE SCIENCE

www.elsevier.com/locate/susc

The interaction of CO_2 and H_2O with Sr films studied with MIES and UPS (HeI)

W. Maus-Friedrichs *, A. Gunhold, M. Frerichs, V. Kempter

Institut für Physik und Physikalische Technologien der Technischen Universität Clausthal, Leibnizstrasse 4, D-38678 Clausthal-Zellerfeld, Germany

Received 22 February 2001; accepted for publication 25 April 2001

Abstract

Metastable impact electron spectroscopy and ultraviolet photoelectron spectroscopy (HeI) were applied to study the interaction of CO_2 and H_2O with Sr films. The films were prepared by evaporating Sr layers (typical thickness: 4 nm) on clean Si(1 0 0). For both CO_2 and H_2O the interaction is initiated by the dissociation of the molecules and the formation of (Sr–O) bonds. Subsequently impinging CO_2 molecules form carbonate complexes CO_3^{2-} involving the (Sr–O) bonds. In the case of H_2O the surface becomes largely covered by hydroxyls at larger exposures. These are formed by hydrogen abstraction from water occurring close to the (Sr–O) bonds.

Keywords: Alkaline earth metals; Carbon dioxide; Water; Insulating films; Corrosion; Metastable induced electron spectroscopy (MIES); Photoelectron spectroscopy

1. Introduction

The interaction of molecules with metals is both of fundamental and of technological interest. In particular, dissociation processes on technologically important surfaces have been studied intensively. The interaction of H_2O [1] and CO_2 [2,3] with metal surfaces is important in corrosion and passivation chemistry. Furthermore, interest in the surface chemistry of CO_2 arises from the catalytic reduction of CO_2 to reduce the green house effect and from the role of CO_2 as a reactant in hydrocarbon synthesis. Many metals and oxides form various types of surface hydroxyl groups, which play a role in chemical surface properties as the catalytic activity [1].

Interest in the investigation of Sr surfaces and its interaction with H_2O, CO_2 and O_2 follows from sensor applications of $SrTiO_3$. Alkaline earth titanates display a macroscopic change in electrical conductivity as a function of the ambient oxygen partial pressure which finds application in high temperature oxygen sensors [4]. In this field $SrTiO_3$ is the most promising candidate due to its temperature stable perovskite structure which remains unchanged from about 100 K up to about 1500 K. Applying different donor and acceptor dopants, first applications as exhaust gas sensors have been implemented [4,5]. Unfortunately, the application of high temperatures (typically up to 1300 K) results in the formation of Sr phases on top of the

* Corresponding author. Tel.: +49-5323-722310; fax: +49-5323-723600.

E-mail address: wmf@physik.tu-clausthal.de (W. Maus-Friedrichs).

0039-6028/01/$ - see front matter
PII: S0039-6028(01)01140-2

surface. The underlying process of the Sr enrichment on $SrTiO_3$ surfaces is the object of intensive investigations, and is, up to now, not well understood. In an oxygen atmosphere [6] and in air [7] Sr layers form (Sr–O) patches. These patches reduce the O_2-sensor efficiency. Typically, a $SrTiO_3$ (1 0 0) surface is covered with 20% SrO islands after heating to 1600 K in an ambient atmosphere for 120 h [7].

With the exception of oxygen (production of heteroepitaxial SrO films on Si(1 0 0) [8]) no results for the interaction of Sr with molecules have been published to our knowledge. It is therefore the intention of our study to give insight into the interaction of Sr layers with H_2O and CO_2 which are components of motorcar exhaust.

2. Experimental techniques

The apparatus is equipped with a cold-cathode gas discharge source for the production of metastable $He^*(2^3S/2^1S)$ ($E^* = 19.8/20.6$ eV) atoms with thermal kinetic energies and HeI photons ($E^* = 21.2$ eV) for ultraviolet photoelectron spectroscopy (UPS). The triplet to singlet ratio amounts to 7:1 [9]. $He^*(2^1S)$ atoms are known to be converted into $He^*(2^3S)$ atoms in front of metallic and semiconducting surfaces very efficiently [10–12]. Therefore almost no contributions induced by $He^*(2^1S)$ atoms are found in the spectra. Metastable and photon contributions within the beam are separated by means of a time of flight technique combined with a twin counter system allowing the simultaneous measurement of metastable impact electron spectroscopy (MIES) and UPS spectra. The angle of incidence of the probe beam is 45° with respect to the surface normal; electrons emitted in the direction normal to the surface are analyzed. The simultaneous collection of a MIES/UPS spectrum requires 100 s. The apparatus is further equipped with a commercial twin-anode X-ray source (Specs model 865) for X-ray photoelectron spectroscopy (XPS). MIES and UPS measurements are performed by using a hemispherical analyzer (VSW HA100) with an energy resolution of 250 meV. All spectra are displayed as a function of the binding energy. Additionally the apparatus is equipped with low energy electron diffraction (Physical Electronics Industries 11-020) and Auger electron spectroscopy (Physical Electronics Industries 11-500A).

MIES and UPS experiments are performed by biasing the target by -50 eV which has been shown to have almost no influence on the spectral features. The Fermi energy (E_F), which corresponds to zero binding energy ($E_B = 0$) is determined from the spectra by electrons emitted from metallic substrates with the maximum kinetic energies. The ejected electrons are detected by the hemispherical analyzer.

Sr layers were produced by evaporating Sr metal (Aldrich, 99.95%) with a commercial UHV metal evaporator (Omicron EFM 3) on a Si(1 0 0) target. The target was cleaned before Sr exposure by heating to about 1000°C for 3 min. Subsequently Sr was evaporated at a rate of about 0.3 Å/s for 150 s at a target temperature below 80°C. Applying this procedure Sr layers with thicknesses of about 4 nm are produced. Layer thickness and evaporation rate were estimated on the basis of XPS and MIES measurements. No emission from the underlying substrate in MIES and UPS (HeI) could be detected for this layer thickness.

CO_2 and H_2O are offered using a bakable UHV leak valve with partial pressures between 2×10^{-9} and 1×10^{-7} mbar. The gas line can be evacuated and cleaned on demand by heating procedures. The UHV pressure is measured using a commercial cold cathode gauge (Pfeiffer MaxiGauge). The partial pressures of the interacting gases can be measured by a quadrupole mass spectrometer (Balzers QMS 112A). To observe the changes of the electronic structure during the gas–surface interaction, gas atoms are offered continuously while MIES and UPS spectra are being collected.

The base pressure of the apparatus is better than 5×10^{-11} mbar; during Sr evaporation the pressure stays below 5×10^{-9} mbar.

Under all studied conditions, i.e. for both the bare Sr and the adsorbate covered Sr surface, the work function stays well below 3.5 eV. Consequently, the MIES spectra are mainly due to the Auger deexcitation process, and a unique relation exists between kinetic energy of the emitted electrons and their binding energies.

3. Results

3.1. Interaction of CO_2 with Sr

Fig. 1 shows the MIES (a) and UPS (b) spectra obtained during the interaction of CO_2 with the Sr layer. The CO_2 exposure increases by 0.2 L per spectrum up to 6 L exposure and in steps of 1 L afterwards ($1\ L = 10^{-6}$ mbar/s). The top spectra correspond to an exposure of 14 L CO_2; the bottom spectra correspond to the pure Sr, respectively.

The work function of (2.7 ± 0.1) eV for the pure Sr layer (as determined by the low energy offset of the spectra) is higher than the work function of Sr(1 0 0) single crystals which amounts to 2.35 eV [13]. At such work functions the $He^*(2^3S)$–surface interaction is normally dominated by Auger deexcitation with possible contributions from the autodetachment process. Auger deexcitation occurs in general for insulators and for metallic surfaces with work functions below 3.5 eV [13,14]. Hereby a surface electron fills the He 1s vacancy emitting the electron in the He 2s orbital by an inter-atomic Auger transition. The emitted electron carries the excess energy. For this process the kinetic energy distribution of the emitted electrons reflects the surface density of states. For work function below about 2.2 eV the resonant transfer of a surface electron into the He 2s orbital becomes probable [15]. The $He^{-*}1s\,2s^2$ ion produced by this transfer decays via a fast autodetachment process into its ground state, emitting one electron from the He 2s orbital. This decay produces an atomic-like line near a kinetic energy of about 19 eV.

For pure Sr a peak is found at a binding energy of (1.4 ± 0.1) eV. For thick Ca layers on Si(1 1 1) the corresponding peak at $E_B = 1.2$ eV was attributed to the Auger deexcitation process involving the Ca(4s) orbitals [16]. Therefore, the main contribution within the observed peak below E_F is thought to arise from the ionization of the Sr(5s) orbitals by Auger deexcitation. The corresponding UPS spectrum is structureless and flat showing the same low kinetic energy onset like the MIES spectra. The Sr DOS consists mostly of a s-derived band with lower contributions from p-derived states, d-states almost do not contribute to the DOS [17]. A strong peak below E_F is therefore not found because the photoionization cross-section for HeI photons with an energy of 21.2 eV and s-orbitals is very low [18].

With increasing CO_2 exposure a peak appears at a binding energy of (5.0 ± 0.1) eV, which is denoted by O_a (O_a denotes surface adsorbed oxygen). This peak is more pronounced with MIES, but is clearly distinguishable with UPS. A similar peak has been found for the interaction of Sr with oxygen in the low coverage range (not shown here). We therefore assume this peak to be due to the formation of a (Sr–O) bond on the surface. This peak will be discussed in Section.4.1.

In MIES and UPS a peak triplet appears at the binding energies $E_B = 6.9$; 11.45; 13.3 eV. These peaks are well known from the ionization of the CO_3^{2-} molecular orbitals ($1a_2'$; $1e''$; $4e'$ corresponding to the peak at $E_B = 6.9$ eV; $3e'$; $1a_2''$ corresponding to the peak at $E_B = 11.45$ eV; $4a'$ corresponding to the peak at $E_B = 13.3$ eV) [19,20]. The same features have been found previously for the interaction of Mg and Ca with CO_2 [16,21,22].

The disappearance of contributions to the spectra in the binding energy range between 0 and 4 eV is characteristic for the formation of an insulating film. The CO_2 covered Sr surface develops a gap between valence band maximum and Fermi energy of about 5.1 eV.

Fig. 2 shows the exposure dependence of the peak intensities of Sr(5s), O_a and the CO_3^{2-} emission at $E_B = 6.9$ eV, together with the change of the surface work function as a function of the CO_2 exposure (from Fig. 1). The work function decreases from its value for the pure Sr layer to a minimum of (2.4 ± 0.1) eV at an exposure around 1 L to its final value of (3.0 ± 0.1) eV for exposures beyond 15 L CO_2. Sr(5s) decreases continuously during CO_2 offer and vanishes around 6 L. O_a reaches its maximum around 1 L together with the work function minimum and has disappeared for exposures beyond about 2.5 L. A strong rise of the carbonate features takes place around the work function minimum.

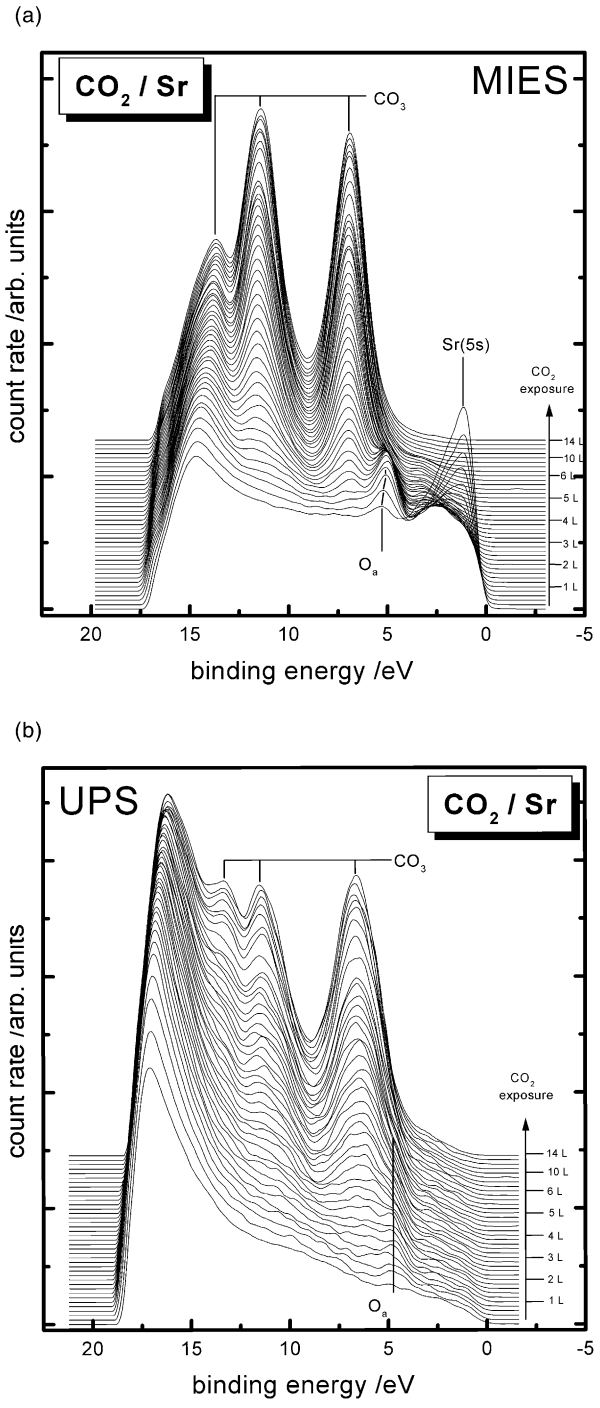

Fig. 1. MIES spectra (a) and UPS spectra (b) of the Sr film during the interaction with CO_2. The respective gas exposures are given with the spectra.

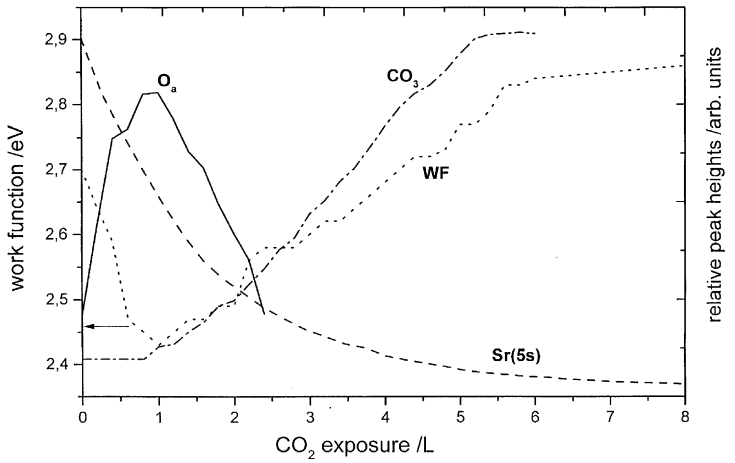

Fig. 2. Exposure dependence of MIES Sr(5s) emission (at $E_B = 1.4$ eV), O_a (peak at $E_B = 5.1$ eV), the surface work function (WF) and the CO_2 intensity (at $E_B = 6.9$ eV) evaluated from Fig. 1.

3.2. Interaction of H_2O with Sr

Fig. 3 shows the MIES (a) and UPS (b) spectra obtained during the interaction of H_2O with the Sr layer. The H_2O exposure increases by 0.2 L per spectrum up to an exposure of 6 L and in steps of 1 L afterwards. The bottom spectra correspond to the pure Sr, the top spectra correspond to an exposure of 18 L, respectively.

As for CO_2, O_a appears at a binding energy of 5.0 ± 0.1 eV in MIES and in UPS. In MIES this peaks starts at $E_B = 6.0$ eV and shifts to about 5.0 eV during H_2O exposure. It is more pronounced in UPS and decreases only slowly compared to MIES.

In MIES and in UPS peaks appear at binding energies $E_B = 7.9$ and 11.8 eV during the H_2O exposure. They correspond to the ionization of OH^- molecular orbitals (1π at $E_B = 7.9$ eV; 3σ at $E_B = 11.8$ eV). Similar peaks were found previously on metals and insulators [1,23,24]. Adsorbed H_2O molecules would produce a peak triplet (typically: $1b_1$ at $E_B = 7.7$ eV; $3a_1$ at $E_B = 9.9$ eV; $1b_2$ at $E_B = 13.3$ eV [1]), which is not observed here. The main difference between hydroxyl and carbonate formation is the appearance of a third peak at large binding energies for CO_2 and also the intensity ratio of the two peaks 1π and 3σ.

For exposures beyond 5 L an additional peak growing at $E_B = 15$ eV is observed in UPS, but not in MIES. For molecular water a peak triplet should appear at $E_B = 7.7$ eV ($1b_1$), 9.9 eV ($3a_1$) and 13.3 eV ($1b_2$) [1]. Especially at 9.9 eV no additional intensity is observed in the spectra; therefore we tend to exclude this feature as being due to molecular water. Contamination from the residual gas could only originate from CO_2. The comparison with the results for the interaction of CO_2 with Sr presented in Section. 3.1 shows that CO_2 can be excluded as source for the additional peak. The observed feature at $E_B = 15.0$ eV could be due to the interaction between the Sr 4p atomic orbital and the OH 1π and, in particular, the 3σ molecular orbitals. For the undisturbed Sr 4p a doublet at $E_B = 20.1$ eV (Sr $4p_{3/2}$) and $E_B = 21.6$ eV (Sr $4p_{1/2}$) is expected [25]. We therefore propose that the observed features at $E_B = 7.9$, 11.8 and 15 eV correspond to the weakest bound states of a (Sr–OH) complex. The two upper states having dominantly 1π and 3σ character while the state at 15 eV has Sr 4p character mainly. In principle, a confirmation of this suggestion could come from HeII measurements, although the expected features might overlap with those in the HeI spectra.

Fig. 4 shows the exposure dependence of Sr(5s), O_a (from MIES and UPS), and the OH 1π emission at $E_B = 7.9$ eV together with the work function as a function of H_2O exposure (from Fig. 3). The data for O_a (MIES and UPS) beyond 1L (3 L)

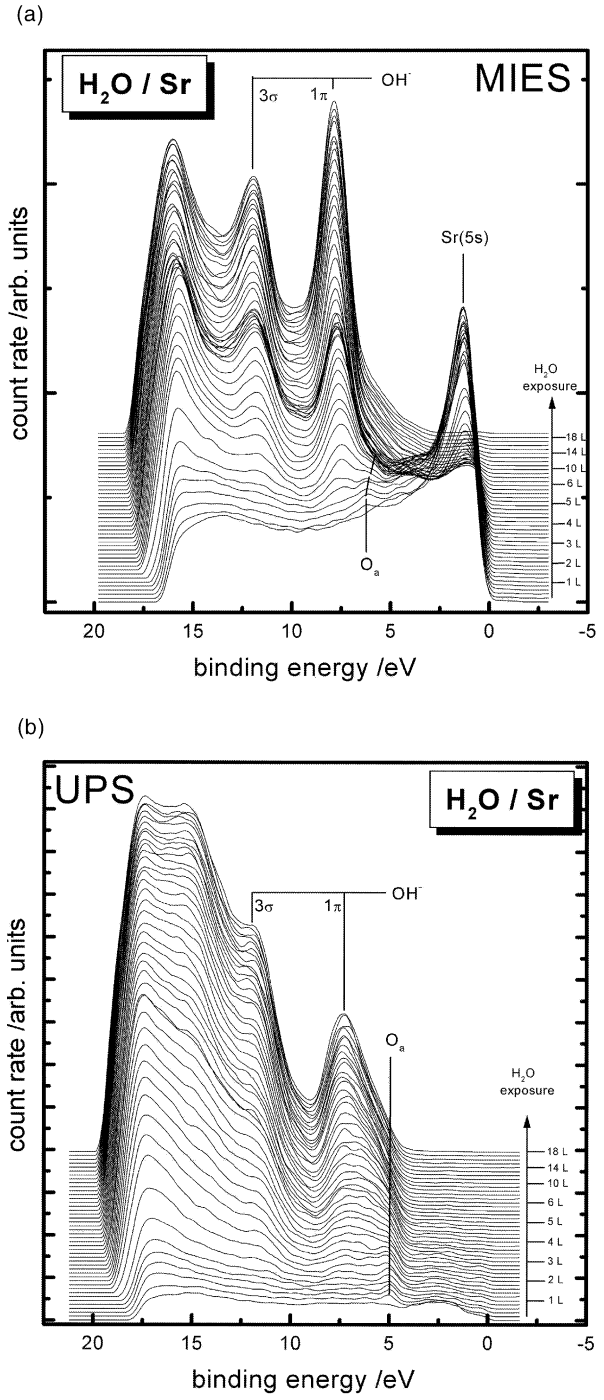

Fig. 3. MIES spectra (a) and UPS spectra (b) of the Sr film during the interaction with H_2O. The respective gas exposures are given with the spectra.

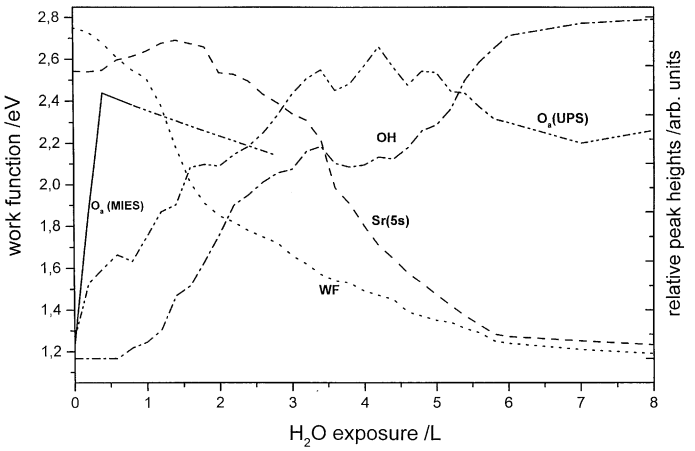

Fig. 4. Exposure dependence of MIES Sr(5s) emission (at $E_B = 1.4$ eV), O_a (peak at $E_B = 5.2$ eV), the surface WF and the OH^- intensity (at $E_B = 7.9$ eV) evaluated from Fig. 3.

for MIES (UPS) are based on the asymmetries of the feature attributed to OH 1π. Therefore the level of confidence is low for larger exposures. However, our interpretation will mainly rely on the low-exposure data. The surface work function decreases continuously and reaches its final value of (1.2 ± 0.1) eV around 8 L H_2O exposure. Beyond 2 L the exposure dependence is difficult to evaluate, but from the asymmetry of the OH 1π feature (as compared to the CO_2 case) it is evident that O_a persists, at least partly, for larger exposures. The MIES OH emission becomes visible at an exposure of about 0.7 L; it saturates around 6 L corresponding with the work function and the disappearance of the Sr(5s) peak.

4. Discussion

4.1. Discussion of O_a

A detailed discussion of the interaction of O_2 with Sr, leading to SrO formation will be the subject of a forthcoming publication [26]. Briefly, during the interaction of both CO_2 and H_2O the feature by O_a is observed. A similar peak is also found during the interaction of Sr with oxygen (not shown here), and is characteristic for the release of O 2p electrons in the metallic environment formed by the surrounding Sr atoms. O 2p electrons from oxygen in an oxide environment are found to have a larger binding energy.

The work function decrease in the initial phase of the O incorporation, which is observed for CO_2, H_2O and also O_2 suggests, that the oxygen is chemisorbed at sites within (or even below) the topmost layer. Indeed, on the basis of ISS results it was found, that on polycrystalline Mg oxygen forms an oxide at sites that are within the outermost Mg layer [27]. Therefore, we conclude that during the initial stage of the interaction of CO_2 and H_2O with Sr, O atoms are produced by the dissociation of the respective molecules forming (Sr–O) bonds.

4.2. Interaction of CO_2 with Sr

For reviews of the surface chemistry of CO_2 the reader is referred to Refs. [2,3]. The following discussion is largely guided by our interpretation of the spectroscopic results obtained for the interaction of CO_2 with Mg and Ca surfaces [16,21, 22]. As in these cases, the CO_2 adsorption is dissociative in the first stage. The presence of O atoms at the surface promotes the bonding of CO_2 as carbonate species. The comparison of the MIES and UPS data shows that the carbonate and oxide species have rather different spatial distributions in the near-surface region with the carbonate being confined to the topmost layer and the oxide

present as an underlayer. As for Mg and Ca the present results are compatible with the following scenario for the interaction of CO_2 with the Sr surface, first proposed in Ref. [28]:

1. impinging CO_2 molecules dissociate in the vicinity of the surface forming (Sr–O) bonds, which manifests themselves as O_a;
2. additional impinging CO_2 molecules chemisorb at the surface oxygen which leads to the CO_3^{2-} termination of the surface.

Fig. 2 shows that the formation of a (Sr–O) bond following the dissociation of CO_2 is a rather fast process as long as the surface has still metallic properties (which is the case as long as the Sr(5s) feature is clearly visible). The metallicity of the surface gradually disappears by the consumption of the Sr valence electrons in forming (Sr–O) bonds. Consequently, the rate of (Sr–O) bond formation decreases and becomes comparable to that for the chemisorption of additional CO_2 at surface oxygen. This leads to the decrease of the O_a peak with increasing exposure.

While the formation of (Sr–O) bonds is leading to a decrease of the work function, the carbonate formation is connected with a rise of the work function. As is shown in [29,30], the CO_2 chemisorption, as a carbonate species, is initiated by the flow of charge from the surface oxygen to the CO_2. The formation of a bent CO_2^--like species facilitates the chemisorption and formation of CO_3^{2-}. Apparently, this charge flow away from the surface is responsible for the work function rise.

The CO_3^{2-} formation ends after the saturation of all (Sr–O) bonds present at the surface. It is evident that the carbonate top layer prevents the Sr film from a further attack of CO_2 molecules.

No emission from CO was found in the spectra. Additional experiments (not shown here) indicate, that CO does not chemisorb on Sr at room temperature.

As far as the properties of $SrTiO_3$ sensors are concerned, the carbonate formation on Sr leads to an insulating character of the surface. This prevents its capability for oxygen dissociation, and therefore reduces its sensitivity.

4.3. Interaction of H_2O with Sr

On the basis of previous results for the water interaction with Mg [31] and BaO [32] and the coadsorption of water and oxygen on metals [1] we propose a model that can account for our findings, in particular the exposure dependence of the spectral features as summarized in Fig. 4. In particular, we note that in the case of Mg the reaction with water at room temperature leads to oxide formation while hydroxyls are being formed at low temperatures [31]. In the case of the water interaction with BaO-complexes formed on W(1 1 0) it was found that BaO patches inhibit the complete water dissociation via $H_2O \rightarrow 2H + O_a$ [32]. On metals, the coadsorption of oxygen and water leads to $(OH)_a$ formation whereby the water dissociation generally appears to proceed via a hydrogen abstraction reaction [1].

We propose that at room temperature water dissociates completely at the bare Sr surface. This leads to the formation of (Sr–O) bonds which are manifesting themselves in the peak at about 5.0 eV (denoted by O_a) on the one hand, and the reduction of the Sr(5s) intensity on the other hand. As for CO_2 the H_2O exposure (below 1 L) leads to the incorporation of oxygen atoms in the Sr layer and to a decrease of the work function. Indeed, complete dissociation of water near room temperature was found on Mg [31]. The decrease in the number of available Sr sites versus exposure is evident from the decrease of the Sr(5s) feature.

$(OH)_a$ accounts for the two features, 1π and 3σ. On the basis of the results for O_2 and H_2O coadsorption on metals [1] we propose that the reaction that forms $(OH)_a$ species is:

$$H_2O + O_a \rightarrow 2(OH)_a$$

whereby the abstracted H atom attaches to the surface oxygen O_a. O_a remains relatively small for all exposures because newly formed (Sr–O) bonds are readily converted into Sr–$(OH)_a$ as a consequence of the H abstraction reaction. In MIES, O_a is particularly small compared to the $(OH)_a$ features, probably because of the geometric shielding of the O_a species by the $(OH)_a$ groups that protrude further into the vacuum. We also note that the sticking coefficient for $(OH)_a$ approaches zero

around 8 L when the Sr(5s) feature from the ionization of the Sr valence electrons has disappeared. Obviously, the surface becomes inert after its has lost its metallic character.

The UPS data suggest that the OH and (Sr–O) bond formation is confined to the uppermost surface layer. The MIES data show, that besides the OH species also some oxygen is present as well in the top layer.

The work function continues to decrease in the exposure range where mainly $(OH)_a$ species are formed (above 1 L). A similar decrease has been observed during OH formation on a MgO surface partially covered by Mg [33]. It is assumed that the work function decrease is related to the reaction of pre-adsorbed Mg with water under the formation of a hydroxide species. Apparently, the similar work function decrease observed for H_2O/Sr is caused by the formation of a hydroxide species, probably $Sr(OH)_2$, at the surface.

The main difference between CO_2 and H_2O interaction with Sr occurs in the reaction step that follows the (Sr–O) formation:

- For CO_2/Sr additional CO_2 chemisorbs at the ($Sr–O_a$) groups forming carbonate-like species.
- For H_2O/Sr additional H_2O chemisorbs at Sr-sites, the (Sr–O) species merely blocking the complete decay of the water.

Similar as discussed for CO_2 the formation of an insulating hydroxide film on Sr patches reduces the sensitivity of $SrTiO_3$ oxygen sensors.

5. Summary

Sr films (typical thickness 4 nm) were produced on Si(1 0 0) surfaces. These films were exposed to CO_2 and H_2O molecules at room temperature. The electronic structure of these films and its modification during exposure were studied with the electron spectroscopic techniques MIES and UPS (HeI).

Sr exposed to CO_2 develops spectral features arising from the ionization of the CO_3^{2-} molecular orbitals. In the first step of the interaction of CO_2 with Sr (Sr–O) bond formation is observed. Additional impinging CO_2 molecules form CO_3 with these (Sr–O) bonds. The mechanism is the same as for the CO_2 interaction with Mg and Ca. A closed carbonate layer is formed on top of the surface after an exposure of 5 L.

Similar to the interaction with CO_2 the formation of (Sr–O) bonds is observed in the initial stage of the H_2O interaction with Sr at room temperature. Complete H_2O dissociation takes place at the metallic Sr surface. For larger exposures the Sr surface develops spectral features corresponding to the ionization of OH 1π and 3σ molecular orbitals. Obviously the presence of (Sr–O) complexes prevents the complete water dissociation. The top layer consists of hydroxyl species mainly.

Acknowledgements

Financial support from the Deutsche Forschungsgemeinschaft within the ''Programm-gruppe: Vom Molekül zum Material'' under contract no. Ma 1893/2-1 is gratefully acknowledged.

References

[1] P.A. Thiel, T.E. Mady, Surf. Sci. Rep. 7 (1987) 211.
[2] F. Solymosi, J. Mol. Catal. 65 (1991) 337.
[3] H.J. Freund, M.V. Roberts, Surf. Sci. Rep. 25 (1996) 225.
[4] W. Menesklou, H.-J. Schreiner, K.H. Härdtl, E. Ivers-Tiffée, Sens. Acuators B 59 (1999) 184.
[5] U. Lampe, J. Gerbliner, H. Meixner, Sens. Actuators B 7 (1992) 787.
[6] K. Szot, W. Speier, U. Breuer, R. Meyer, J. Szade, R. Waser, Surf. Sci. 460 (2000) 112.
[7] H. Wei, L. Beuermann, J. Helmbold, G. Borchardt, V. Kempter, G. Lilienkamp, W. Maus-Friedrichs, J. Electroceram. Soc. (2001), in press.
[8] H. Asaoka, K. Saiki, A. Koma, H. Yamamoto, Thin Solid Films 369 (2000) 273.
[9] D. Ochs, W. Maus-Friedrichs, M. Brause, J. Günster, V. Kempter, V. Puchin, L. Kantorovich, A. Shluger, Surf. Sci. 365 (1996) 557.
[10] J. Lee, C. Hanrahan, J. Arias, F. Bozso, R.M. Martin, H. Metiu, Phys. Rev. Lett. 54 (1985) 1440.
[11] B. Woratschek, W. Sesselmann, J. Küppers, G. Ertl, H. Haberland, Phys. Rev. Lett. 55 (1985) 611.
[12] A.G. Borisov, D. Teillet-Billy, J.P. Gauyacq, Surf. Sci. 284 (1993) 337.

[13] G. Ertl, J. Küppers, Low Energy Electrons and Surface Chemistry, VCH Verlagsgesellschaft, Weinheim, 1985.
[14] Y. Harada, S. Masuda, H. Ozaki, Chem. Rev. 97 (1997) 1897.
[15] R. Hemmen, H. Conrad, Phys. Rev. Lett. 67 (1991) 1314.
[16] D. Ochs, B. Braun, W. Maus-Friedrichs, V. Kempter, Surf. Sci. 417 (1998) 406.
[17] D.A. Papaconstantopoulos, Handbook of the Band Structure of Elemental Solids, Plenum Press, New York, 1986.
[18] J. Günster, Th. Mayer, V. Kempter, Surf. Sci. 359 (1996) 155 and references there in.
[19] Y. Fukuda, I. Toyoshima, Surf. Sci. 158 (1994) 837.
[20] Y. Harada, H. Ozaki, Jpn. J. Appl. Phys. 26 (1987) 1201.
[21] D. Ochs, M. Brause, B. Braun, W. Maus-Friedrichs, V. Kempter, Surf. Sci. 397 (1998) 101.
[22] D. Ochs, M. Brause, W. Maus-Friedrichs, V. Kempter, J. Electron. Spectrosc. Rel. Phenom 88–91 (1998) 757.
[23] D.S. Toledano, P. Metcalf, V.E. Henrich, Surf. Sci. 472 (2001) 21.
[24] J. Günster, S. Krischok, J. Stultz, D.W. Goodman, J. Phys. Chem. B 104 (2000) 7977.
[25] http://www.webelements.com/webelements/elements/text/Sr/bind.html.
[26] W. Maus-Friedrichs, A. Gunhold, M. Frerichs, V. Kempter, in press.
[27] J.A. Schultz, M.H. Mintz, T.R. Schuler, J.W. Rabalais, Surf. Sci. 146 (1984) 438.
[28] S. Campbell, P. Hollins, E. McCash, M.W. Roberts, J. Electron. Spectrosc. Rel. Phenom. 145 (1986) 145.
[29] G. Pacchioni, Surf. Sci. 281 (1993) 207.
[30] G. Pacchioni, J.M. Ricart, F. Illas, J. Am. Chem. Soc. 116 (1994) 10152.
[31] J. Fuggle, Surf. Sci. 49 (1975) 61.
[32] D. Mueller, A. Shih, J. Vac. Sci. Technol. A 6 (1988) 1067.
[33] J. Günster, S. Krischok, V. Kempter, D.W. Goodman, Chem. Rev. (2001), in press.